the chains of III atoms running along the c axis, giving rise to alternating bonds of 2·78 and 2·89 Å. Except for a shortening of the shortest bond, the bond-length histogram of Fig. 7 is very similar to that given by Donohue (1974). The exception arises because Donohue chose the value $z = \frac{3}{4}$ for atom III, giving two bonds of 2·83 Å along the c axis. Our experiment proves that there are two short bond lengths.

Conclusion and summary

The principal result of our investigation is the demonstration that the β-phase of uranium has the centrosymmetric space group $P4_2/mnm$. The previous controversies (Donohue, 1974) are thereby resolved. The choice of space group depends mainly, although not completely, on the determination of certain z coordinates. For these investigations we have used neutrons (for which the absorption is very small) with a high-resolution diffractometer and the Rietveld profile method to increase the accuracy of the refined parameters. A powder sample was used to minimize the effects of grain growth and texture, and the background from the fused silica container was effectively removed (Richardson & Faber, 1986). All these methods are advances over those used in the original X-ray studies performed prior to 1970, and some confidence may be placed in the new results. Unfortunately, we still do not know why the structure of β-uranium is as complicated as it is, and the reasons for this complexity of structure remain one of the major unsolved problems in the crystal chemistry and physics of the actinide elements.

We wish to thank J. Faber Jr, R. L. Hitterman, F. J. Rotella and A. Severing for much advice and experimental assistance, and we are especially grateful to D. Wozniak for his help with the construction and calibration of the furnaces. Both ANL and LANL are supported by the US Department of Energy. IPNS is operated by the Basic Energy Sciences Division of USDOE as a National User Facility.

References

ARAI, M. (1984). IPNS Note 27. Argonne National Laboratory, Argonne, USA.

BARRETT, C. S., MUELLER, M. H. & HITTERMAN, R. L. (1963). *Phys. Rev.* **129**, 625–629.

BAUR, W. H. & TILLMANS, E. (1986). *Acta Cryst.* B**42**, 95–111.

BERGMAN, G. & SHOEMAKER, D. P. (1954). *Acta Cryst.* **7**, 857–865.

BROOKS, M. S. S., JOHANSSON, B. & SKRIVER, H. K. (1984). In *Handbook of the Physics and Chemistry of the Actinides*, Vol. 1, edited by A. J. FREEMAN & G. H. LANDER, p. 153 *et seq.* Amsterdam: North-Holland.

CHIOTTI, P., KLEPFER, H. H. & WHITE, R. W. (1959). *Trans. Am. Soc. Met.* **51**, 772–778.

DONOHUE, J. (1974). *The Structures of the Elements*, pp. 134–148. New York: John Wiley.

DONOHUE, J. & EINSPAHR, M. (1971). *Acta Cryst.* B**27**, 1740–1743.

DUWEZ, P. (1953). *J. Appl. Phys.* **24**, 152–154.

HOLDEN, A. N. (1958). *Physical Metallurgy of Uranium*, pp. 30–32. Reading, Massachusetts: Addison-Wesley.

JORGENSEN, J. D. & FABER, J. JR (1982). In *Proceedings of ICANS VI*, Report 82-80, edited by J. M. CARPENTER, pp. 105–112. Argonne National Laboratory, Argonne, USA.

JORGENSEN, J. D. & ROTELLA, F. J. (1982). *J. Appl. Cryst.* **15**, 27–32.

LANDER, G. H. & MUELLER, M. H. (1970). *Acta Cryst.* B**26**, 129–136.

MARSH, R. E. (1986). *Acta Cryst.* B**42**, 193–198.

MUELLER, M. H., HITTERMAN, R. L. & KNOTT, H. W. (1962). *Acta Cryst.* **15**, 421–422.

PEARSON, W. B. (1972). *The Crystal Chemistry and Physics of Metals and Alloys*, p. 675. New York: Wiley–Interscience.

PEIERLS, R. (1955). *Quantum Theory of Solids*, pp. 108–112. Oxford Univ. Press.

RICHARDSON, J. W. JR & FABER, J. JR (1986). In *Advances in X-ray Analysis*, edited by C. S. BARRETT, J. B. COHEN, J. FABER JR, R. JENKINS, D. E. LEYDEN, J. C. RUSS & P. K. PREDECKI, Vol. 29, pp. 143–152. New York: Plenum Press.

RIETVELD, H. M. (1969). *J. Appl. Cryst.* **2**, 65–69.

SMITH, H. G. & LANDER, G. H. (1984). *Phys. Rev. B*, **30**, 5407–5415.

VON DREELE, R. B., JORGENSEN, J. D. & WINDSOR, C. G. (1982). *J. Appl. Cryst.* **15**, 581–589.

Acta Cryst. (1988). B**44**, 96–101

Electron Density in Non-Ideal Metal Complexes. IV. Hexaaquametal(II) Ammonium Sulfates

BY E. N. MASLEN, S. C. RIDOUT AND K. J. WATSON

Department of Physics, University of Western Australia, Nedlands, Western Australia 6009, *Australia*

(*Received* 7 *February* 1987; *accepted* 29 *October* 1987)

Abstract

The electron-density distributions in $(NH_4)_2M^{II}(SO_4)_2 \cdot 6H_2O$, with M = Mg and Ni are compared. Both magnesium and nickel densities show approximate 4*mmm* symmetry, consistent with the geometries of the structures. The distributions near the metal atoms are similar, except for differences which can be understood in terms of the d electrons in the nickel structure. For the shortest nickel–oxygen bond there is a deep

0108-7681/88/020096-06$03.00

minimum in the deformation density 0·6 Å from the metal nucleus. This is consistent with exchange. The nickel map, which indicates strong polarization of the *d*-electron density, also shows evidence of orbital mixing associated with the departure from octahedral geometry. This cannot be due to the hydrogen-bond system, which is similar for the ligating water molecules. It originates in longer range interactions between Ni atoms and ammonium groups in the next coordination sphere.

Introduction

Varghese & Maslen (1985) and Maslen & Ridout (1987), in papers I and III of this series, studied second-order effects in the charge density for non-ideal transition-metal compounds. These structures were selected because they contain departures from ideality which have significant effects on the electron density. The work of Marumo, Isobe, Saito, Yagi & Akimoto (1974) and of Marumo, Isobe & Akimoto (1977) has shown that a change of atom type in an isomorphous series can have a significant effect on residual electron density.

The hexaaquametal(II) ammonium sulfates form an isomorphous series of complexes known as Tutton's salts. The symmetry of the hexaaquametal ion is close to octahedral for a wide range of metals. The ion cannot be exactly octahedral, since the water molecule has *mm*2 symmetry, and not 4*mm* as required for exact octahedral coordination.

In this paper we report electron-density studies on Tutton's salts containing magnesium and nickel. For the Mg^{2+} ion, which contains no 3*d* electrons, the prepared state is spherically symmetric, whereas that for the Ni^{2+} ion, which has an incomplete 3*d* subshell, will be non-spherical if the populations of the t_{2g} and e_g orbitals differ from their free-atom values. The geometries for the two structures including the hydrogen-bond networks, which are described by Maslen, Ridout, Watson & Moore (1988*a*,*b*), are closely similar. The magnesium complex serves as a reference system which allows the effects of including the *d* electrons to be assessed.

An earlier charge-density study on the nickel Tutton's salt was reported by Treushnikov, Kuskov, Soboleva & Belov (1978) who, while mainly concerned with the sulfate group, also observed an asymmetric charge distribution near the Ni atom.

The X-ray data for the new charge-density studies were used to refine the structures. Details of the data collection and refinements are reported by Maslen, Ridout, Watson & Moore (1988*a*,*b*).

Electron density

The exact symmetry of the metal-atom site is $\bar{1}$, but the geometry of the metal–oxygen vectors is approximately octahedral, and more closely 4/*mmm* (D_{4h}), with *M*—O(9) along the unique axis. The *M*—O(9) bond length is 0·03 Å shorter than the *M*—O(7) and *M*—O(8) values, which are similar to each other. If this difference resulted from the hydrogen bonding of the ligating waters the hydrogen-bond system involving O(9) would differ from those involving O(7) and O(8). However, the hydrogen-bond lengths involving O(9) resemble those for O(8), which differ from those for O(7). This suggests that the distortion from the ideal octahedral geometry originates in another type of interaction in the structure. The electron density was analysed to help identify that interaction.

Table 1. *Atomic charges, as defined by Hirshfeld* (1977)

$[NH_4]_2[Mg(H_2O)_6](SO_4)_2$			$[NH_4]_2[Ni(H_2O)_6](SO_4)_2$		
Atom	Group	Charge	Atom	Group	Charge
Mg		0·28 (3)	Ni		0·05 (3)
O(7)		0·05 (3)	O(7)		0·01 (3)
H(15)		−0·02 (2)	H(15)		0·06 (2)
H(16)		0·02 (2)	H(16)		0·03 (2)
	H_2O	0·05		H_2O	0·09
O(8)		0·01 (3)	O(8)		−0·09 (3)
H(17)		0·04 (2)	H(17)		0·03 (2)
H(18)		0·05 (2)	H(18)		−0·04 (2)
	H_2O	0·10		H_2O	−0·11
O(9)		0·02 (3)	O(9)		0·10 (3)
H(19)		0·05 (2)	H(19)		0·08 (2)
H(20)		0·08 (2)	H(20)		0·04 (2)
	H_2O	0·16		H_2O	0·22
	$Mg(H_2O)_6$	0·91		$Ni(H_2O)_6$	0·45
N(10)		0·30 (3)	N(10)		0·30 (3)
H(11)		0·05 (2)	H(11)		0·16 (2)
H(12)		0·03 (2)	H(12)		0·07 (2)
H(13)		0·09 (2)	H(13)		0·17 (2)
H(14)		0·15 (2)	H(14)		0·09 (2)
	NH_4	0·61		NH_4	0·80
S(2)		0·27 (3)	S(2)		0·21 (3)
O(3)		−0·36 (3)	O(3)		−0·28 (3)
O(4)		−0·32 (3)	O(4)		−0·43 (3)
O(5)		−0·35 (3)	O(5)		−0·22 (3)
O(6)		−0·33 (3)	O(6)		−0·36 (3)
	SO_4	−1·10		SO_4	−1·08

Structure factors were evaluated using the neutron parameters for the H atoms and those from the X-ray analysis for the remaining atoms. The difference density for each structure was evaluated. Atomic charges, determined by the method of Hirshfeld (1977) using the program *PARTN* (Chantler, 1985), are given in Table 1. The standard deviations were derived by approximating the density distribution for each atom by that in a sphere of equivalent volume, following the method of Davis & Maslen (1978).

For the magnesium structure the charges for chemically related atoms are consistent within the standard deviations. Although the charges for the two structures are similar, the internal agreement between charges for the nickel structure is less satisfactory. This is not unexpected, in view of the dominance of the nickel core scattering for the nickel structure. The fact that this is not reflected in the standard deviations for the charges suggests that the $\sigma|F_o|$ values for the low-angle structure factors, which predominantly determine the charges, are underestimated. This may be related to the

amount of extinction, which is larger for the nickel structure.

The largest charges on individual atoms are less than 0·5 electrons, those on the metal cations being markedly lower than the formal value of +2. The positive charge on the Mg atom is larger than that on the Ni atom – a result consistent with the chemical behaviour of the two metals.

The charge on each group is between about half and one times the formal value. This is in contrast with the values for the individual atoms, for which the charges are smaller. The positive charge on the water molecule containing O(9) is larger than those on the waters containing O(7) and O(8) – a trend which continues through the Tutton's salt series (Maslen & Watson, 1987).

The consistency of the charges, and their relationship to the chemical properties of the functional groups, confirms that the difference densities contain chemical information. Values of $\sigma(\Delta\rho)$, determined using the formula of Rees (1977) for the benefit of those who consider such point estimates to be a useful guide to accuracy, are 0·10 and 0·09 e Å^{-3} for the magnesium and nickel structures respectively.

Sections of the residual density for planes containing the metal and the three sets of four co-planar O atoms are shown in Figs. 1 and 2 for magnesium and nickel respectively. The first diagram in each set, labelled (*a*), which contains the *M*—O(7) and *M*—O(8) bonds, would have 4*m* symmetry if the 4/*mmm* symmetry were exact. As far as the electron density near the metal is concerned the *M*—O(7) and *M*—O(8) vectors are almost equivalent. The symmetries of both maps are close to 4*m*. The (*b*) and (*c*) maps have lower symmetry.

The approximate symmetry of these maps, being consistent with the ligand geometry, differs from that of the hydrogen-bond system, as noted above. Thus the effect of the hydrogen bonding of the ligand waters on the electron density near the metal is not significant.

The features in the $\Delta\rho$ map near the Ni atom are more pronounced than those near the Mg, reflecting the high polarizability of the 3*d* electrons for the Ni atom. This is confirmed by the arrangement of the principal maxima and minima, which correspond to excess t_{2g} occupancy and reduced e_g occupancy for the 3*d* electrons in the nickel map.

It was observed in papers I and III that the lone pairs near O atoms bonded to metal atoms were weakly localized, and this is also true in the present structures. This holds especially for O(9). There is less positive electron density along the short *M*—O(9) than there is along the *M*—O(7) and *M*—O(8) bonds. This is reflected in the atomic charges from Table 1.

There are minima $0{\cdot}3_5$ Å from the metal centre along the Ni—O(7) and Ni—O(8) vectors, whereas a ridge of weakly positive density straddles the metal centre along the Ni—O(9) vector. There is a deep hollow along that vector, but it lies at the end of the ridge and reaches a minimum 0·6 Å from the metal. In the maps for the magnesium complex (Fig. 1) there is a similar ridge along the Mg—O(9) vector. Although the polarization is weaker there are regions of negative density along Mg—O(7), Mg—O(8) and Mg—O(9) corresponding to the deeper minima along Ni—O(7), Ni—O(8) and Ni—O(9) in Fig. 2.

Thus notwithstanding the lack of 3*d* electrons for magnesium, there are marked similarities between the magnesium and nickel maps. The anisotropy of the electron density near the nuclei is similar in both cases. This reinforces a conclusion from paper I, namely that the anisotropy of the electron density near the nucleus may be more reliable than is generally recognized. The correspondence indicates that the metal atoms are subject to similar ligand fields.

The polarization indicated by the depletion in the Ni—O(9) direction is far greater than that along the Ni—O(7) and Ni—O(8) bonds, which are only 0·03 Å longer. The proximity of the metal and O(9) nuclei implies reduced screening of the nuclei, and hence higher potential, along the *M*—O(9) bond. Simple electrostatic arguments do not account for this minimum which is the most significant feature in the nickel difference map. The deformation density for the closely related copper structure has similar characteristics (Maslen, Watson & Moore, 1988). That is, for a metal with a nearly filled *d* subshell, there is strong depletion of electron density in volume elements directed towards an electron-rich ligand. The depletion of the oxygen lone-pair density along the direction of the *M*—O(9) bonds in the magnesium and nickel structures must also be explained.

A number of authors (*e.g.* Bader, 1981) argue against such depletion of electron density in chemical bonds, by stressing reasons for increase in the density in the bond. The Hellmann–Feynman theorem is used to justify the claim that an increase of the density between chemically bonded atoms is the norm, since depletion of density produces a repulsive force on the nuclei. Such arguments are simply not relevant to the case of a metal with symmetrical coordination.

Forces on the metal owing to depletion of density near the nucleus cancel by symmetry. In this context it should be noted that symmetrical coordination with electronegative ligands is strongly favoured by metals with nearly filled *d* subshells.

While the result cannot be accounted for in terms of electrostatic forces on a classical electron-charge cloud some of its characteristics are as predicted by the Pauli exclusion principle. When an electron-rich ligand, such as a water oxygen, intrudes on the *d* subshell, electrons with parallel spins overlap. Depletion of the electron density in the subshell is a direct consequence of antisymmetrizing the wavefunction, *i.e.* of exchange.

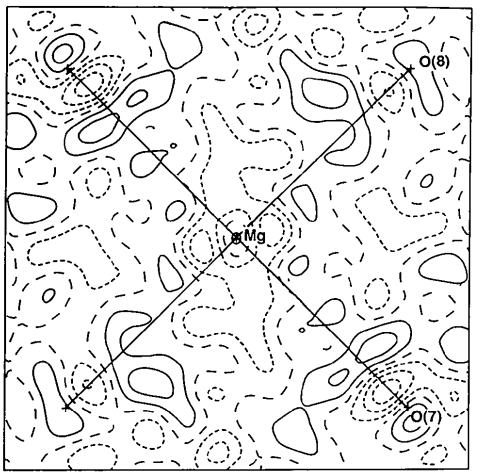

(*a*)

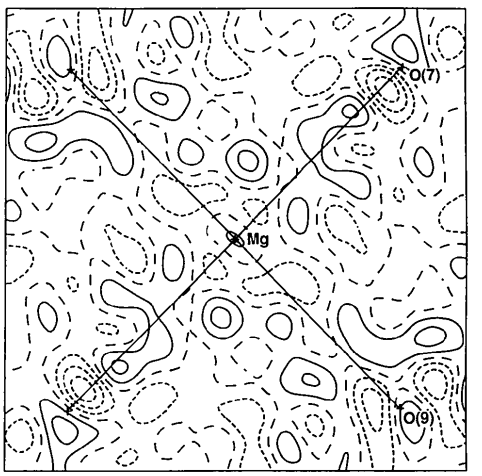

(*b*)

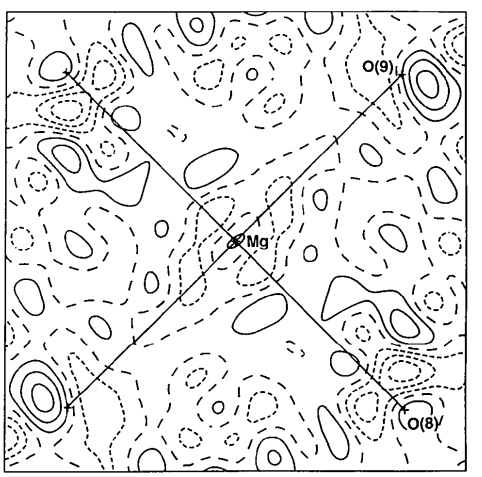

(*c*)

Fig. 1. Residual density for the magnesium structure in (*a*) the Mg–O(7)–O(8) plane, (*b*) the Mg–O(7)–O(9) plane and (*c*) the Mg–O(8)–O(9) plane. Contour interval 0·15 e Å^{-3}. Zero contour broken. Negative contours dotted.

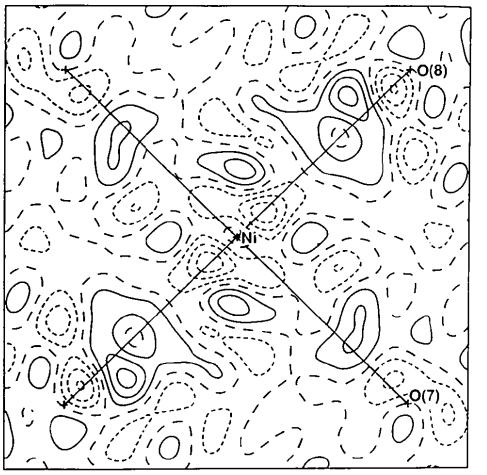

(*a*)

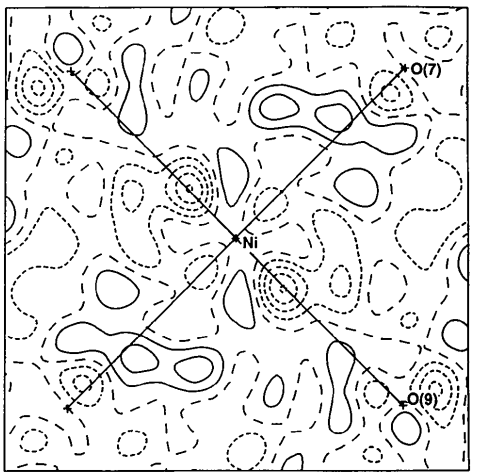

(*b*)

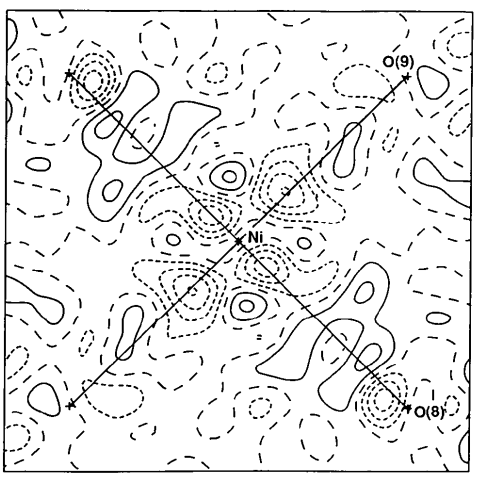

(*c*)

Fig. 2. Residual density for the nickel structure in (*a*) the Ni–O(7)–O(8) plane, (*b*) the Ni–O(7)–O(9) plane and (*c*) the Ni–O(8)–O(9) plane. Contours as for Fig. 1.

However the differences in the lengths of the M—O(7), M—O(8) and M—O(9) bonds are quite small, and cannot affect the exchange potential dramatically. They cannot explain the qualitative difference in the topography of the $\Delta\rho$ map near the Ni—O(7), Ni—O(8) and Ni—O(9) bonds in Fig. 2.

Since the topography of the $\Delta\rho$ map cannot be attributed to factors within the hexaaquanickel moiety alone, or to its hydrogen-bond environment, we are obliged to consider the effects of interactions in the next coordination sphere. Typical distances between the Ni atom and neighbouring ammonium groups (represented by the central N atom) and the atoms in the sulfate groups are shown in Fig. 3. This is a projection of the structure down the c axis, which is aligned roughly (within 25°) along the M—O(9) bond.

There are four pairs of interaction vectors with ammonium groups and four pairs with sulfate groups at distances (measured from the central atom in the group) less than 6·0 Å from the metal atom. Table 2 lists the components of these vectors on local axes related to the geometry of the hexaaqua moiety. The table includes the sums of the magnitudes of these components weighted inversely as the square of the length for each vector. For each ligand these sums are similar with one exception – the low value of the components for the ammonium groups along the M—O(9) vector. This reflects the proximity of the ammonium group to O(7) and O(8), as seen in Fig. 3.

Whereas the order of the other totals in Table 2 can be varied by extending the cut-off radius to include

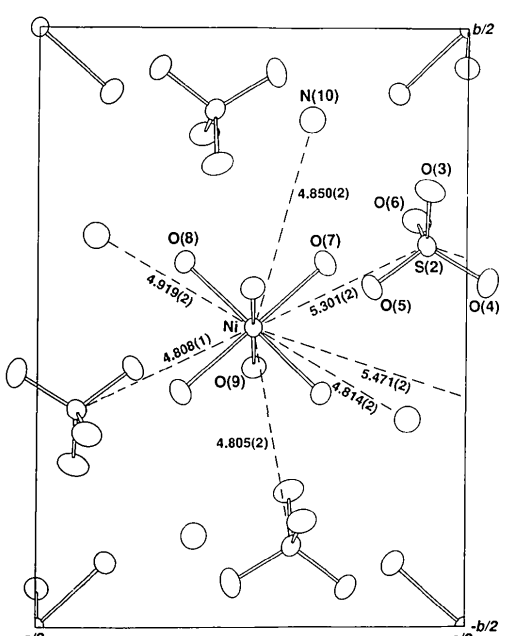

Fig. 3. Projection of the structure down the c axis showing vectors from the Ni atom to ammonium groups and S atoms, with distances in Å.

Table 2. *Coordinates of central atoms for groups adjacent to the hexaaquanickel moiety* (Å)

The coordinates are defined by the ligating water O atoms. R is the distance from the central Ni atom. Sum refers to totals of magnitudes of components, weighted by R^{-2}, for each atom type.

	x	y	z	R
O(7)	2·06	0·06	0·00	2·068
O(8)	0·00	2·06	0·00	2·066
O(9)	0·00	0·02	2·04	2·037
Sum	0·48	0·50	0·49	
S(2^{i})	−1·88	−3·12	3·14	4·805
S(2^{ii})	−2·96	2·16	3·10	4·808
S(2)	4·62	−0·22	2·58	5·301
S(2^{iii})	2·76	−4·66	0·84	5·471
Sum	0·47	0·39	0·39	
N(10^{iv})	1·96	−2·50	3·62	4·814
N(10)	4·08	2·64	−0·04	4·850
N(10^{ii})	0·30	4·46	2·08	4·919
N(10^{v})	5·42	−2·36	−0·20	5·916
Sum	0·43	0·48	0·25	

Equivalent positions: (i) $-\frac{1}{2}+x, \frac{1}{2}-y, -1+z$; (ii) $-x, -y, 1-z$; (iii) $1-x, -y, 1-z$; (iv) $-\frac{1}{2}+x, \frac{1}{2}-y, z$; (v) $\frac{1}{2}+x, \frac{1}{2}-y, z$.

further interactions, the sum of the projections of the M—NH_4 vectors onto the M—O(9) vector remains low. The two shortest N—O distances, 3·17 and 3·27 Å, involve O(8) and O(7) respectively. The Ni—O—N angles involving those vectors, 138·7 and 129·4° respectively, are similar. The orientation of the water molecules favours interaction between the ammonium group and the lone pair of the water oxygen which is not involved in the M—O bond. Thus the location of the ammonium group accounts for the lengthening of the M—O(7) and M—O(8) bonds.

The main difference between the magnesium and nickel maps are features associated with the nickel d electrons. The appearance of Fig. 2(c) is striking in that the maxima associated with increased t_{2g} occupancy are rather small, but these are accompanied by satellites displaced approximately $0{\cdot}6_5$ Å from the d-electron peaks in a direction normal to, and radially outwards from, the Ni—O(9) bond. Sections containing the Ni—O(9) vector, and bisecting the angle between Ni—O(7) and Ni—O(8) are shown in Fig. 4. There are strong satellite maxima only for Fig. 4(a), which contains the internal bisector of the angle between the two Ni—O bonds.

The origin of similar satellites for a cobalt complex is discussed in paper III. They are not prominent in structures with ideal geometry – and indeed they do not occur in Fig. 2(a), which has near to 4m symmetry. They appear to be a manifestation of orbital mixing which occurs when the symmetry is lower than that expected for pure d orbitals.

Relative to molecular axes defined by the M—O(7), M—O(8) and O(9) vectors, the idealized directions for the interactions with the metal atom are [1$\bar{1}$1], [210], [021] and [2$\bar{1}$0] for the ammonium groups and [$\bar{1}\bar{1}$1], [$\bar{1}$11], [201] and [1$\bar{2}$0] for the S atoms. Strong satellite

maxima occur consistently only in the directions pointing towards the ammonium groups, and their heights are 0·1 e Å^{-3} higher than any which are directed towards the sulfate groups. The satellites are particularly prominent in the Ni–O(8)–O(9) plane (Fig. 2*c*). Two of the three shortest vectors to the ammonium groups are close to this plane.

The effect is illustrated in Fig. 4. The Ni–N(10) vector, of length 4·850 Å, is approximately normal to the Ni–O(9) bond and lies close to the plane of Fig. 4(*a*), which has well developed satellite peaks pointing towards the ammonium group. Near the plane of Fig. 4(*b*), which does not contain an interaction vector normal to the Ni–O(9) bond, any satellites are of marginal significance.

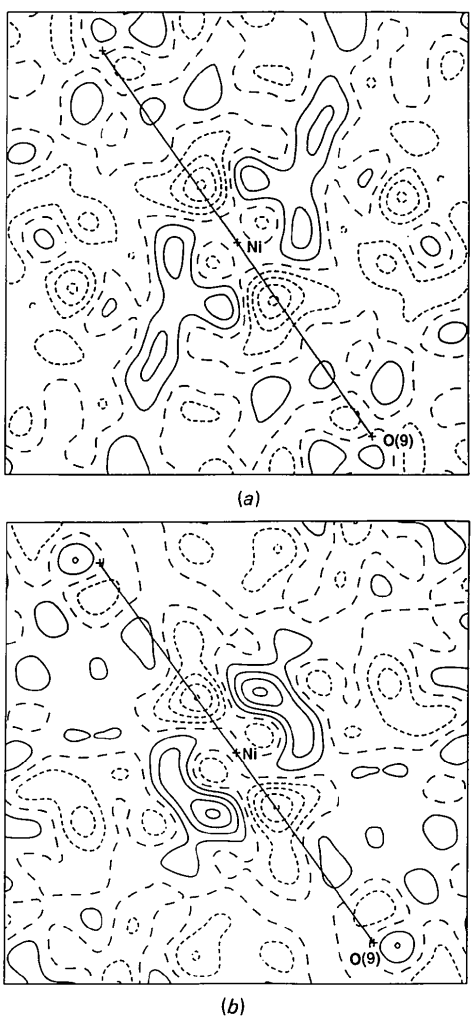

Fig. 4. Residual density for the nickel structure in planes containing Ni–O(9) and bisecting the angles between the Ni–O(7) and Ni–O(8) vectors. Sections containing (*a*) the internal bisector and (*b*) the external bisector. Contours as for Fig. 1.

If the effects of interactions with second-nearest neighbours were small, the deformation densities for the two sections shown in Fig. 4 would be similar, since both contain the Ni–O(9) vector and a bisector of the O(7)–Ni–O(8) angle. There is a marked difference in the topography of the deformation density in the two sections, showing the effect of the second-nearest-neighbour interactions.

Because chemical bonding is predominantly a short-range phenomenon, it is widely believed that the effect of longer range interactions on electron density is minimal. Evidence for significant contributions to the residual density associated with longer range forces have now been obtained in a number of structures (Maslen, Spadaccini & Watson, 1983, 1986; Varghese & Maslen, 1985; Maslen & Ridout, 1987). The validity of assuming that residual density is always dominated by short-range bonding effects must be questioned.

Thanks are due to A. H. White for measurement of the X-ray data. This work was supported by the Australia Research Grants Scheme and by the University of Western Australia Research Committee. Extensive use was made of the programs *FOURR, SLANT, CONTUR* and *PLOT* from the *XTAL* system (Stewart & Hall, 1985).

References

BADER, R. F. W. (1981). *The Force Concept in Chemistry,* edited by B. M. DEB, pp. 39–136. New York: Van Nostrand–Reinhold.
CHANTLER, C. (1985). *PARTN* program – listing and documentation. Unpublished work.
DAVIS, C. L. & MASLEN, E. N. (1978). *Acta Cryst.* A**34**, 743–746.
HIRSHFELD, F. (1977). *Theor. Chim. Acta,* **44**, 129–138.
MARUMO, F., ISOBE, M. & AKIMOTO, S. (1977). *Acta Cryst.* B**33**, 713–716.
MARUMO, F., ISOBE, M., SAITO, Y., YAGI, T. & AKIMOTO, S. (1974). *Acta Cryst.* B**30**, 1904–1906.
MASLEN, E. N. & RIDOUT, S. C. (1987). *Acta Cryst.* B**43**, 352–356.
MASLEN, E. N., RIDOUT, S. C., WATSON, K. J. & MOORE, F. H. (1988*a*). *Acta Cryst.* C**44**, 409–412.
MASLEN, E. N., RIDOUT, S. C., WATSON, K. J. & MOORE, F. H. (1988*b*). *Acta Cryst.* C**44**, 412–415.
MASLEN, E. N., SPADACCINI, N. & WATSON, K. J. (1983). *Proc. Indian Acad. Sci.* **92**, 443–448.
MASLEN, E. N., SPADACCINI, N. & WATSON, K. J. (1986). *Acta Cryst.* B**42**, 430–436.
MASLEN, E. N. & WATSON, K. J. (1987). Unpublished work.
MASLEN, E. N., WATSON, K. J. & MOORE, F. H. (1988). *Acta Cryst.* B**44**, 102–107.
REES, B. (1977). *Isr. J. Chem.* **16**, 180–186.
STEWART, J. M. & HALL, S. R. (1985). *The XTAL System of Crystallographic Programs. User's Manual.* Univ. of Maryland, College Park, Maryland, USA.
TREUSHNIKOV, E. N., KUSKOV, V. I., SOBOLEVA, L. V. & BELOV, N. V. (1978). *Kristallografiya,* **23**, 30–41.
VARGHESE, J. N. & MASLEN, E. N. (1985). *Acta Cryst.* B**41**, 184–190.